Effective Inhibition of c-MET-mediated Signaling, Growth, and Migration of Ovarian Cancer Cells is Influenced by the Ovarian Tissue Microenvironment

Youngjoo Kwon[1,2], **Bryan D Smith**[3], **Yan Zhou**[4], **Michael D Kaufman**[3], and **Andrew K Godwin**[1,5]

[1]Department of Pathology and Laboratory Medicine, University of Kansas Medical Center, Seoul, Korea

[2]Department of Food Science and Engineering, Ewha Womans University, Seoul, Korea

[3]Deciphera Pharmaceuticals, LLC, Lawrence, KS 66044

[4]Biostatistics and Bioinformatics Facility, Fox Chase Cancer Center, Philadelphia, Pennsylvania, USA

[5]University of Kansas Cancer Center, Kansas City, KS, USA

Abstract

The signaling mediated by c-MET and its ligand, hepatocyte growth factor (HGF), has been implicated in malignant progression of cancer involving stimulation of proliferation, invasion, and metastasis. We studied the c-MET/HGF axis as a mediator of tumor-stromal interaction in ovarian cancer and the value of targeting c-MET for the treatment of ovarian cancer. To assess c-MET signaling, we established *in vitro* models of the microenvironment using primary and immortalized human fibroblasts from normal ovary and tumor samples and epithelial ovarian cancer cell lines. We found that fibroblast from normal ovaries secreted high levels of HGF (1,500 to 3,800 pg/mL) as compared to tumor-derived fibroblasts (undetectable level) and could elicit cellular biological responses on c-MET expressing ovarian cancer cells including increase of cell proliferation and migration (2- to 140-fold increase). HGF secreted by fibroblasts was also found sequestered within extracellular matrices (ECMs) and when degraded this ECM-derived HGF stimulated cancer cell migration (1.5- to 24-fold). In cells containing constitutive c-MET phosphorylation, recombinant HGF and fibroblast-derived HGF negligibly affect c-MET phosphorylation on Tyr^{1234} and Tyr^{1003}. However, both sources of HGF increased the phosphorylation of c-MET on Tyr^{1349}, the multi-substrate docking site, by more than 6-fold and led to activation of downstream signaling transducers. DCC-2701 (Deciphera Pharmaceuticals,

Corresponding author: Andrew K. Godwin, Ph.D., Department of Pathology and Laboratory Medicine, University of Kansas Medical Center, Mail Stop 3040, 3901 Rainbow Blvd, Kansas City, KS 66160, AGodwin@kumc.edu.

Author Manuscript

LLC), a novel c-MET/TIE-2/VEGFR inhibitor was able to effectively reduce tumor burden *in vivo* and block c-MET pTyr[1349]-mediated signaling, cell growth, and migration as compared to a HGF antagonist *in vitro*. Importantly, DCC-2701's anti-proliferative activity was dependent on c-MET activation induced by stromal human fibroblasts and to a lesser extent exogenous HGF. Our data suggest for the first time that DCC-2701 may be superior to HGF antagonists that are in clinical trials and that pTyr[1349] levels might be a good indicator of c-MET activation and likely response to targeted therapy as a result of signals from the microenvironment.

Keywords

INTRODUCTION

Epithelial ovarian cancer has the highest mortality rate of all gynecologic malignancies diagnosed in the U.S. (1). Rapid progression of ovarian cancer without symptoms makes this disease deadly and difficult to clinically manage (2).

Stromal cells play a significant role in malignant progression of cancer (3, 4). In particular, fibroblasts and their derived extracellular matrices (ECMs) compose a large part of stroma and are associated with cancer cells at all stages of cancer development (5). Fibroblasts secrete many paracrine signalling factors that promote proliferation, invasion, and migration of cancer cells (3, 4). Those growth factors secreted by fibroblasts are incorporated into the ECM and can transduce signals to cancer cells without being released (solid-phase ligands) or following degradation of the ECM and their release (6). Therefore, stromal components in the ovary might be important contributors of rapid progression of ovarian cancer and interruption of their interaction with cancer cells may be an important therapeutic target.

Among many stromal growth factors, hepatocyte growth factor (HGF) is expressed mainly in mesenchymal cells and acts on epithelial cells (7, 8). This epithelial-stromal relationship of c-MET and HGF was reported in normal ovary as well (9). HGF is also one of the known growth factors that can bind to extracellular matrix proteins or proteoglycans (10, 11), thereby being sequestered within ECMs to elicit biological responses when it is necessary. More importantly, HGF is a unique cytokine that induces pleiotropic biological responses, involving proliferation, invasion, and dissemination of cancer cells (7, 12). Recent reports reiterate a significant role of fibroblast-derived HGF in mediating disease progression as well as immediate innate resistance to targeted therapies (13, 14). In addition, overexpression of c-MET, the only known receptor for HGF, has been reported in many cancers of epithelial cell origin including ovarian cancer (12, 15).

The versatile biological effect of c-MET/HGF signalling made it an attractive therapeutic target and many small molecules of c-MET kinase inhibitors and antibodies targeting HGF or c-MET have been developed. Encouragingly, targeting c-MET using PF-2341066 (16) or foretinib, a multikinase inhibitor (17), exhibited effective anti-tumor activities against ovarian cancer in animal models. However, no anti-tumor effect was observed in an ovarian cancer clinical trial conducted using AMG-102, humanized IgG$_2$ directed against HGF,

capable of preventing HGF binding to c-MET and subsequent c-MET activation (12, 18, 19). This disappointing clinical outcome might be due to the ineffective penetration of antibody-based drug into tumors, the inability to completely sequester ligand, and/or that c-MET activation may be independent of HGF in ovarian cancer.

In this study, we evaluated c-MET and HGF signalling as a mediator of stromal-cancer cell interaction in ovarian cancer using human ovarian fibroblast and their derived ECMs. We evaluated a novel c-MET/TIE-2/VEGFR inhibitor, DCC-2701, and assessed its ability to inhibit the HGF/c-MET axis stimulated by stromal-cancer cell interactions. We report that human ovarian fibroblasts secrete HGF that lead to increased growth and migration of ovarian cancer cells. HGF that was sequestered within fibroblast-produced ECMs was also functional upon degradation of the ECM by tumor cells. Fibroblast-derived HGF increased the c-MET phosphorylation on Tyr^{1349} and cells with maximum activation of c-MET were more susceptible to drug inhibition.

RESULTS

Ovarian cancer cells exhibit enhanced migration by interaction with ovarian fibroblasts and their derived ECMs

A transwell co-culture system was used to evaluate the effect of factors secreted by fibroblasts or released from fibroblast-derived ECMs on ovarian cancer cell migration. Ovarian cancer cells were allowed to migrate in the presence of different fibroblasts and their derived ECMs. Ovarian cancer cells were not highly migratory without the signals produced by ovarian fibroblasts with the exception of SKOV3 cells (Figure 1a), e.g., immortalized human fibroblasts from normal ovaries (IHFNO-303 fibroblasts) enhanced migration by more than 30-, 4-, 20-, 140-, and 1.9-fold in OVCAR3, OVCAR4, OVCAR5, PEO1, and SKOV3, respectively. In comparison, OVCAR10 cells did not respond to fibroblast signals (Figure 1a). OVCAR3, OVCAR4 and SKOV3 cells exclusively showed increased migration in the presence of IHFNO-303 while other fibroblasts, IHFNO-402 and IHFOT-208, could also promote the migration of OVCAR5 and PEO1 cells (Figure 1a). Cells exhibiting significantly enhanced migration in response to IHFNO-303 fibroblasts also exhibited significantly increased ($p < 0.05$) migration in the presence of IHFNO-303 derived matrix (Figure 1a & b). Increase of cell migration was modest or minimal by the interaction with ECMs derived from IHFNO-402 and IHFOT-208 (IHFNO-402M and IHFOT-208M, respectively).

HGF is a major stromal growth factor that contributes to the enhanced cell migration by fibroblasts

In order to determine the factor(s) that promotes migration of ovarian cancer cells, we evaluated a larger panel of growth factors and cytokines (data not shown). Only one of the growth factors, HGF, corresponded to the migration patterns seen in Figure 1. Therefore, HGF levels were further established by ELISA from fibroblast- and ECM-conditioned media in the presence and absence of ovarian cancer cells. As shown in Figure 2a, HGF concentration was significantly higher in conditioned media derived from IHFNO-303 and IHFNO-303M (average of 3,800 pg/mL and 800 pg/mL, respectively) compared to serum

free or standard media. None of the cancer cells produced detectable level of HGF with the exception of OVCAR10 cells that secreted 620 pg/mL of HGF (Figure 2a). We also obtained conditioned media from primary fibroblasts derived from normal ovaries and ovarian tumors and measured HGF levels. In human fibroblasts derived from normal ovaries (HFNO-), 4 out of 6 fibroblasts secreted high level of HGF (1,500 to 2,200 pg/mL), but none of the fibroblasts derived from ovarian tumors (HFOT-) secreted measurable HGF levels (Figure 2b). The levels of HGF secreted by primary ovarian fibroblasts were comparable to their immortalized counterpart (Figure 2a & b). Similarly, HGF levels were high in the stromal compartment of normal ovaries (Supplementary Figure S1) and lower in the tumor stroma, although some tumor samples with extensive stromal components expressed high levels of HGF (Supplementary Figure S1).

We next evaluated if extraneously added recombinant human HGF induces a similar migratory response in ovarian cancer cells. All the cells responsive to IHFNO-303 fibroblast and IHFNO-303M enhanced their migration upon exposure to recombinant HGF (100 ng/mL) with 3-, 4-, 9-, 11-, and 1.6-fold increase in OVCAR3, OVCAR4, OVCAR5, PEO1, and SKOV3 cells, respectively, compared to their basal levels (Figure 2c). This HGF-induced cell migration was effectively inhibited by a HGF neutralizing antibody (Figure 2c), making no significant difference compared to non-stimulated cells. As observed with fibroblasts (Figure 1a), recombinant HGF did not enhance the migration of OVCAR10 cells (Figure 2c). Therefore, ovarian cancer cells responded to recombinant HGF similarly to IHFNO-303 fibroblast (4 ng/mL of HGF level) but required higher levels; e.g., 25 times more recombinant HGF was required to achieve similar increase of OVCAR4 migration by IHFNO-303 fibroblasts (Figure 2c and Supplementary Figure S2) and SKOV3 cells (Figure 2c). In OVCAR5 cells, recombinant HGF-induced migration was lower at all concentrations tested (2 to 200 ng/mL) compared to IHFNO-3O3 fibroblast and was not further enhanced by increasing the concentration more than 100 ng/mL (Supplementary Figure S2). These results suggest the possible contribution by other secretory factors produced by the fibroblasts. Nevertheless, cancer cell migration stimulated by IHFNO-303 fibroblast and IHFNO-303M were effectively blocked by a HGF neutralizing antibody in all responsive cells (Figure 2d), further supporting that fibroblast-derived HGF is the primary growth factor contributing to the enhanced cell migration. The same concentration of IgG antibody did not affect cell migration (Supplementary Figure S3).

In order to examine other factors that might affect cell migration promoted by HGF, recombinant HGF was added to the conditioned media of IHFNO-402 and IHFOT-208; two fibroblast lines that produce undetectable levels of HGF and that weakly induce tumor cell migration (Figure 1). Interestingly, a dramatic enhancement of HGF-induced migration (Supplementary Figure S4a) was observed for both OVCAR5 and PEO1 cells (>2.5- and 8-fold, respectively). This finding suggests that common secretory factors derived from fibroblasts might affect cell migration induced by recombinant HGF. It is well established that HGF binds to glycosaminoglycan (GAGs) such as heparan sulfate (HS) (20) and this type of post-translational modification can alter the biological activity of HGF (21, 22). Therefore, we examined whether HS can modulate cell migration induced by recombinant HGF in ovarian tumor cells. We observed that cell migration was reduced by the treatment of IHFNO-303 CM with heparanse III which cleaves HS (Supplementary Figure S4b), while

the addition of exogenous HS along with recombinant HGF enhanced migration in OVCAR5 cells (Supplementary Figure S4c). HS itself did not affect the cell migration and the migration enhanced by the addition of HS was effectively suppressed by a HGF neutralizing antibody (Supplementary Figure S4d), suggesting that stimulation of migration attributed by HS is dependent on the presence of HGF.

c-MET expression levels were measured in the ovarian cancer cells and compared with their migratory response to HGF. OVCAR3, OVCAR4, OVCAR5, PEO1, and SKOV3 cells that migrated in response to IHFNO-303, IHFNO-303M, and recombinant HGF expressed c-MET but OVCAR10 cells which were non-responsive to any source of HGF did not (Figure 2e). Some cancer cells, e.g., OVCAR5 and PEO1 cells, highly expressed phosphorylated c-MET on $Tyr^{1234/1235}$ and Tyr^{1003} but their constitutive level on Tyr^{1349} was relatively low or undetectable (Figure 2e). c-MET expressing cancer cells also increased their cell proliferation in response to recombinant HGF (Supplementary Figure S5).

Conditioned media derived from migration-inducing fibroblasts and recombinant HGF similarly activate c-MET signaling

We next examined that IHFNO-303 conditioned media (IHFNO-303 CM) containing fibroblast-derived HGF and recombinant HGF similarly induce c-MET signaling in ovarian cancer cells that express c-MET. In OVCAR4 cells, c-MET was not phosphorylated without HGF (Figure 3). All tested c-MET phosphorylation sites, $Tyr^{1234/1235}$, Tyr^{1003}, and Tyr^{1349}, were phosphorylated upon exposure to both IHFNO-303 CM and recombinant HGF but not IHFOT-208 CM which contains undetectable level of HGF (Figure 2a). Phosphorylation of c-MET (all three sites) was detected as early as 5 min following treatment and reached the maximum level between 30 min to 2 hr and lasted until 24 hr. OVCAR4 cells constitutively expressed p-AKT and p-ERK at low levels but the increase of phosphorylation on both AKT and ERK was apparent 30 min after treating cells with either source of HGF and lasted until 24 hr. IHFOT-208 CM appeared to also activate AKT and ERK independent of c-MET and to a lesser degree compared to IHFNO-303, suggesting the presence of additional stimulatory growth factors secreted by the fibroblasts. Similar patterns of c-MET activation in response to IHFNO-303 CM, recombinant HGF, and IHFOT-208 CM were observed in OVCAR3 and SKOV3 cell lines (Supplementary Figure S6). However, AKT and ERK activation induced by HGF was less apparent in cells with constitutively high level of p-AKT and p-ERK and therefore, phosphorylation of AKT and ERK might not be a good indicator of c-MET activation. In OVCAR5 cells where c-MET is constitutively phosphorylated (Figures 2e & 3), phosphorylation levels on $Tyr^{1234/1235}$ and Tyr^{1003} were not affected by IHFNO-303 CM although their levels were further elevated by recombinant HGF. In contrast, phosphorylation of c-MET on Tyr^{1349} was highly induced by both IHFNO-303 CM and HGF, subsequently increasing both p-AKT and p-ERK levels. Similar patterns were observed in PEO1 cells that also possess constitutive c-MET phosphorylation (Supplementary Figure S6).

DCC-2701, a small molecule of c-MET inhibitor, effectively inhibits c-MET activation induced by HGF-providing microenvironment

The effect of DCC-2701, a novel c-MET/TIE-2 inhibitor currently in development (23) was tested on c-MET-mediated signal transduction in OVCAR5 and PEO1 cells that constitutively express phosphorylated c-MET. Cells were treated with serum free media or IHFNO-303 CM containing DCC-2701 at concentrations ranging from 0 to 5 μM for 1 hr. Both constitutive (serum free) and HGF-induced (IHFNO-303 CM) c-MET phosphorylation was effectively inhibited by DCC-2701 in OVCAR5 and PEO1 cells (Figure 4). DCC-2701 acted on all three phosphorylation sites tested, $Tyr^{1234/1235}$, Tyr^{1003}, and Tyr^{1349} (Figure 4). It is noteworthy that c-MET on Tyr^{1349}, the multisubstrate docking site, was highly induced by physiological HGF and the HGF-induced phosphorylation was effectively inhibited by DCC-2701. It was apparent that inhibition of phosphorylation on Tyr^{1349} by DCC-2701 resulted in subsequent suppression of AKT phosphorylation in a dose dependent manner in OVCAR5 cells (Figure 4). The p-ERK level was not greatly affected by the drug treatment (Figure 4) probably because these cells contain constitutively high expression of p-ERK.

Next, we examined the extent of c-MET inhibition by DCC-2701 over time. OVCAR5 and PEO1 cells were maintained in serum free media or IHFNO-303 CM containing 1.25 μM DCC-2701, a concentration sufficient to block the phosphorylation of all three c-MET phosphorylation sites (Figure 4) for varying time periods up to 24 hr. Cells were also treated with IHFNO-303 CM containing a HGF neutralizing antibody (2.5 μg/mL) to compare the effect of two different types of c-MET/HGF inhibitors on c-MET signaling. DCC-2701 completely blocked both constitutive and induced c-MET phosphorylation at all tested sites for up to 24 hr in OVCAR5 and PEO1 cells (Figure 5). The effect of DCC-2701 was more apparent on cells cultured with IHFNO-303 CM (HGF-provided by stromal microenvironment), completely abrogating c-MET Tyr^{1349} phosphorylation. In this physiological condition, DCC-2701 effectively blocked the activation of c-MET and subsequently inhibited phosphorylation of AKT induced by IHFNO-303 CM in OVCAR5 cells over 24 hr (Figure 5). In comparison, the HGF neutralizing antibody was not effective in inhibiting activation of c-MET and its downstream effectors (Figure 5) probably due to its function of sequestering secreted HGF rather than directly inhibiting c-MET activity.

DCC-2701 reduces the cell viability and migration capability activated by the HGF-providing microenvironment

To evaluate the effect of DCC-2701 on ovarian cancer cell growth, cells were cultured within standard media or IHFNO-303 CM containing DCC-2701 in a concentration range from 0 to 10 μM. Cell growth rate for 72 hr was estimated using the CellTiter Blue reagent. DCC-2701 reduced the viability of ovarian cancer cells maintained in standard media, but at high concentrations of drug (Figure 6a). Cell viability was more effectively reduced by DCC-2701 when c-MET was maximally activated by IHFNO-303 CM; IC_{50} values 2 ~ 3 fold less when compared to standard media (Figure 6a). DCC-2701 at concentration of 2.5 μM inhibited cell viability by over 70% in IHFNO-303 CM compared to about 10% in standard media in OVCAR5 and PEO1 cells that possess constitutive c-MET phosphorylation ($Tyr^{1234/1235}$, Tyr^{1003} but not Tyr^{1349}). IHFNO-303 CM increased cell viability in varying degree depending on cell lines, higher in OVCAR3, OVCAR4,

OVCAR5, and PEO1 (30–60%) and relatively lower in OVCAR10 and SKOV3 (10–20%) (data not shown). In order to test whether the greater effect of DCC-2701 within IHFNO-303 CM is due to the HGF-induced activation of c-MET, similar experiment was conducted using standard media containing recombinant HGF (100 ng/mL) in OVCAR5 and OVCAR10 cells that represent c-MET positive and negative cells, respectively. IC_{50} value of DCC-2701 was 1.3-fold lowered in OVCAR5 cells by the addition of HGF in the standard media whereas no difference was observed in OVCAR10 cells (Figure 6b). The addition of a HGF neutralizing antibody (0.5 to 4 μg/mL) into IHFNO-303 CM did not change the cell viability in OVCAR5, PEO1, and SKOV3 cells tested (Supplementary Figure S7). DCC-2701 also significantly inhibited cell migration induced by IHFNO-303 CM in OVCAR5 and SKOV3 cells at lower concentrations than required to inhibit cell viability (Figure 6c). Although DCC-2701 has activity against, VEGFR2, none of the lines tested expressed detectable level of the receptor (data not shown).

DCC-2701 effectively reduces ovarian tumor growth *in vivo*

A xenograft nude mouse model, generated by subcutaneous inoculation of SKOV3 cells was used to examine the anti-tumor effects of DCC-2701. After 28 days of treatment, the tumor burden was significantly decreased by an average of 53% and 52% in DCC-2701 treatment groups 10 and 20 mg/kg, respectively relative to the vehicle-treated control group ($p < 0.05$) (Figure 7). The toxicities of DCC-2701 was also assessed by monitoring body weight, mortality unrelated to tumor, and clinical signs of mice in each treatment group. The doses and schedules in the study did not cause discernible adverse effects for DCC-2701, as shown by no significant loss (< 20%) of body weight (Supplemental Figure S8). No general signs of toxicity were noted at necropsies of all remaining mice at the end of the study among all groups (data not shown).

DISCUSSION

The c-MET/HGF axis has been an attractive therapeutic target in many types of cancers. In ovarian cancer, cancer cells overexpress c-MET and high expression of c-MET is related with an adverse prognosis (24). Moreover, some c-MET inhibitors tested (e.g., PF-2341066 and foretinib) effectively inhibited ovarian cancer development and metastases in animal models (16, 17), implicating that the c-MET/HGF axis is a promising target in human ovarian cancer. However, ovarian cancer patients did not benefit from the monotherapy of AMG102 (a humanized HGF antagonising antibody), rendering early termination of the trial (Martin personal communication). This discouraging result might be due to inefficient penetration of the antibody and/or possible ligand-independent activation of c-MET in ovarian cancer. These potential limitations in targeting HGF and delivery of antibody-based therapy suggest that small molecule inhibitors targeting c-MET might be a better approach. Therefore, we evaluated the activity of DCC-2701, a c-MET/TIE-2/VEGFR inhibitor on ovarian cancer cell growth and migration. Given that c-MET and HGF typically act in a paracrine manner, it is important to understand c-MET regulation and evaluate c-MET inhibitors within the physiologically relevant microenvironment. We used human ovarian fibroblasts and their derived ECMs to exploit the interaction of c-MET and HGF within physiological context.

Most ovarian cancer cell lines tested expressed c-MET. Interestingly, c-MET expression was limited to cells that possess epithelial cell characteristics (25) while the cells presenting mesenchymal phenotypes such as OVCAR10 lacked expression (Figure 2e). In agreement with our observation, A2780 cells that fall into mesenchymal cell category (25) did not express c-MET (24).

Constitutive c-MET phosphorylation was observed in some ovarian cancer cells, e.g., OVCAR5 and PEO1, (Figure 2e) where the effect of IHFNO-303 CM was minimal on c-MET phosphorylation sites, $Tyr^{1234/1235}$ and Tyr^{1003} (Figure 3 & Supplementary Figure S6). In comparison to cells constitutively expressing phosphorylated c-MET, phosphorylation on $Tyr^{1234/1235}$ and Tyr^{1003} were highly induced upon exposure to IHFNO-303 CM in OVCAR3, OVCAR4, and SKOV3 cells that do not constitutively express phosphorylated c-MET. More importantly, regardless of constitutive c-MET phosphorylation status, IHFNO-303 CM greatly enhanced the level of c-MET phosphorylation on Tyr^{1349} and subsequently increased the phosphorylation of downstream signal transducers, e.g. AKT and ERK (Figure 3 & Supplementary Figure S6). Phosphorylation of Tyr^{1349} and Tyr^{1365} in the carboxy-terminal tail creates a docking site for the recruitment of multiple transducers and adaptors and therefore, is critical for activation of downstream signaling (12, 26–28). Thus, our results suggest that ovarian cancer cells with constitutively active c-MET, can be further stimulated via stromal derived HGF. These results correlate with the dramatic increase of cell migration in response to IHFNO-303 (fibroblast that secrete high level of HGF) and IHFNO-303M (ECMs derived from IHFNO-303) in all cancer cells that express c-MET (Figures 1a & 2d). This is also in agreement with the observation that c-MET activating mutations still depend on active HGF to acquire their catalytic activity (29). In addition, it is important to point out that in cells that possess constitutive c-MET phosphorylation, the level of phosphorylation on Tyr^{1349} is a better indicator of c-MET activation as a result of stromal-epithelial cells interactions, which is in agreement with a previous report (30).

Importantly, our studies suggested for the first time that c-MET targeted therapies maybe more effective when c-MET is activated by stromal interactions (Figures 4 & 5). This is in agreement with great increase of phosphorylated levels of c-MET on Tyr^{1349} and subsequent increase of p-AKT and p-ERK levels under HGF-providing microenvironment (Figure 3) and therefore, making cells more dependent on c-MET activity for their growth (data not shown). DCC-2701 at the higher concentration (>5 μM) led to decreased cell viability in OVCAR10 cells that are negative for c-MET expression, suggesting DCC-2701 might have some off-target effect at non-physiologic concentrations. However, at lower concentrations (~1 μM) the effect of DCC-2701 appeared to be limited to c-MET expressing cells that are maximally activated. Interestingly, in OVCAR5 and PEO1 cells that contain constitutive phosphorylated c-MET, DCC-2701 (2.5 μM) inhibited cell viability by over 70 % in IHFNO-303 CM compared to about 10% in standard media. Greater effect of DCC-2701 treatment within the HGF-provided condition might partially explain why response to many c-MET targeting small molecules did not correlate well with c-MET level alone (19). The HGF neutralizing antibody was only able to suppress the c-MET activation to the constitutive level or higher and did not effectively abolish the induction of AKT phosphorylation in OVCAR5 cells (Figure 5) and did not affect cell viability. Therefore, our

study suggests that the antibody-based therapy may not completely inhibit c-MET activation and that partial inhibition might be sufficient to reduce cell migration (Figure 2d) but has little effect on cell viability (Supplementary Figure S7).

Furthermore, we found that not all fibroblasts secreted high amount of HGF or have pre-deposited trapped HGF within the ECM (Figure 2a & b). In our studies fibroblasts that secrete high level of HGF were all derived from normal ovary but not from ovarian tumors. Tumor-derived fibroblasts (e.g. IHFOT-208) secreted HGF but measurable amounts were detected only after concentrating their conditioned media (data not shown). We do not know whether those fibroblasts produce less HGF or have defect of secretion as seen in fibroblasts derived from pulmonary fibrosis (31). Similarly, stromal HGF levels were high in normal ovaries *in vivo* (Supplementary Figure S1). High levels of HGF was also observed in some tumor stroma (Supplementary Figure S1), but most noticeably in tumors that possess a high proportion of stroma relative to tumor cells. Perhaps these tumor-associated fibroblasts are part of the "invasive front" and that upregulation of c-MET activity in the tumor cells at the invasive front contributes to the invasive phenotype. Another important finding from our studies is that HGF derived from fibroblast was sequestered within ECMs (Figure 2a) and ECM-derived HGF triggered the same biological response (Figure 2d). Recombinant HGF can bind to ECMs, and proteases (e.g., urokinase-type plasminogen activators, MMPs) can release and activate ECM-bound HGF (32). We speculate that incubating cells within a 3D matrix at 37°C may induce some degree of protease-mediated ECM degradation which causes the release of bound HGF (25). In addition, serine proteases and/or MMPs secreted by cancer cells (25) might further increase the release of ECM-bound HGF and activation of released HGF. This is the first experimental demonstration that HGF produced by fibroblast is stored within ECMs and elicits biological response in interaction with cancer cells. Binding of HGF to ECMs may be an important mechanism to enrich HGF in a local area and provide the complexity of c-MET regulation (6). These results suggest that proteolytic release of HGF from the ECM at the invasive front could provide a gradient for tumor invasion at the border with normal tissue.

A caveat of our study was that exogenous HGF alone could not fully reproduce the biological activities observed for fibroblast-conditioned media. For example IHFNO-303 enhanced tumor cell migration by 2- to 140-fold; however, migration induced by recombinant HGF alone was significantly lower (Figure 2c & d). This observation suggests that other factors in the conditioned medium might cooperate with HGF to induce migration. We speculated that post-translational modification of HGF by glycosaminoglycan such as heparan sulphate (HS) might contribute to this difference. It has been reported that HGF can bind to HS (20, 33) and that the subsequent modifications could alter the biological activity of HGF in wound healing and mitogenic activity (22, 34). As such we demonstrated that treatment of HGF with HS could alter the cell migration capability of ovarian tumor cells induced by recombinant HGF (Supplementary Figure S4). Although exogenously added HS and HGF was inferior to the induction induced by fibroblast-conditioned media and HGF, our results imply that post-translational modifications of growth factors such as HGF might be one mechanism to promote tumor growth via factors produced by the microenvironment. In addition, different sources of HS have different binding activity to HGF (21), suggesting

that HS derived from fibroblast may have a critical structural domain for the binding of HGF. Thus, our data suggest that fibroblasts also secrete factors such as HS that can modify the biological activity (e.g., stimulatory effect on cell migration) of HGF and further contribute to tumor progression; however, additional proteomic based studies will be required to fully characterize tumor-associated modifications of HGF.

In conclusion, ovarian cancer cells, regardless of their constitutive activated c-MET levels, can be further stimulated via stromal derived HGF. The biological response induced by this physiological HGF was effectively inhibited by a novel c-MET inhibitor, DCC-2701 *in vitro* as well as in a xenograft mouse model of ovarian cancer. Overall, these studies suggest the potential clinical value of DCC-2701 for the treatment of patients with ovarian cancers that are dependent on or addicted to c-MET activity for their growth and that pTyr[1349] levels might be a good indicator of c-MET activation and likely response to targeted therapy as a result of signals from the microenvironment.

MATERIALS AND METHODS

Cell cultures and fibroblast-derived ECM production

Ovarian cancer cell lines, OVCAR3, OVCAR4, OVCAR5, OVCAR10, PEO1, and SKOV3 (35, 36) were maintained in RPMI 1640 medium supplemented with 10% fetal bovine serum (FBS), 0.3 U/mL insulin, 2 mM L-glutamine, 100 U/mL penicillin, and 100 μg/mL streptomycin. Primary fibroblasts (e.g. HFNO-303, HFNO-402, and HFOT-208) were obtained as previously described (37) from human ovarian tissues or ovarian tumors under a protocol approved by the FCCC institutional review board. Immortalized lines of HFNO-303, HFNO-402, and HFOT-208 (IHFNO-303, IHFNO-402, and IHFOT-208, respectively) were derived by stably introducing human telomerase reverse transcriptase (hTERT) and subculturing for more than 30 passages. Fibroblasts were evaluated for their mesenchymal characteristics; e.g., negative for keratin and positive for α-smooth muscle actin (α-SMA), vimentin (Supplementary Figure S9). Fibroblasts were cultured in Dulbecco's modified Eagle's medium supplemented with 10% FBS, 2 mM L-glutamine, 100 U/mL penicillin, and 100 μg/mL streptomycin. Cells were cultured in a humidified incubator at 37 °C and 5% CO_2. All the reagents formulated for media were purchased from Mediatech, Inc. (Manassas, VA) except for insulin (Life Technologies, Grand Island, NY). *In vivo*-like 3D matrices were produced from immortalized fibroblast lines in 24-well plate (50,000 cells per well), as previously described (38–41) and stored in phosphate buffered saline at 4°C until used for both migration assay and measurement of HGF concentration by ELISA.

Antibodies and drugs

Antibodies used for c-MET/HGF signaling were phospho-c-MET[Y1234/1235], phospho-c-MET[Y1003], phospho-c-MET[Y1349], c-MET, phospho-AKT[S473], AKT, phospho-ERK1/2, ERK1/2, and GAPDH. All the above antibodies were purchased from Cell Signaling Technology, Inc. (Danvers, MA). Anti-pan-keratin (Abcam Inc., Cambridge, MA), anti-vimentin (Sigma-Aldrich, St. Louis, MO), and anti-α-SMA (Sigma-Aldrich) were used to ensure the purity and fibroblast-like phenotype of isolated fibroblasts. Anti-HGF (goat

antibody) and goat IgG were purchased from R & D Systems Inc. (Minneapolis, MN) and used as a HGF neutralizer or a negative control, respectively. Human recombinant HGF was purchased from R & D Systems. A small molecule of c-MET inhibitor, DCC-2701, was kindly gifted by Daniel Flynn (Deciphera Pharmaceuticals, LLC. Lawrence, KS). Heparan sulfate and heparase III were purchased from Sigma-Aldrich.

Cell migration assay

The migration capacity of cancer cells was estimated using 24-well Transwell plates with polycarbonate membranes (Corning Inc., Corning, NY). Ovarian cancer cells (40,000 cells/ well) were plated on the membrane (upper well). Prior to plating cancer cells, fibroblasts (125,000 cells/well) were plated in the lower well and 24 hr after seeding, their media were changed into serum free media and conditioned for 24 hr. Similarly, ECMs derived from different fibroblasts produced (in the lower well) and stored were conditioned under serum free media for 24 hr at 37°C before plating cancer cells. Whenever necessary, recombinant human HGF and HGF neutralizing antibody were added at the lower well 1 hr before plating cancer cells. For DCC-2701 drug treatment, both ovarian cancer cells and lower wells were treated with the vehicle control (DMSO) or drug for 1 hr before assembling upper and lower wells. Cells were allowed to migrate for 24 hr and the cells remaining in the top of the membrane were gently removed using a cotton swab. Cells migrated onto the bottom side were fixed and nuclei were stained with Hoechst 33342 (Sigma-Aldrich). Random nine fields of stained nuclei per membrane were imaged at 10 X using Nikon 80i fluorescent microscope (Nikon Inc., Melville, NY) equipped with image acquisition and processing software, MetaMorph (Molecular Devices, Downingtown, PA). The number of nuclei in each field was counted and averaged. Data were expressed as mean ± SE from three independent experiments.

Cell viability assay

Ovarian cancer cells (2,000–3,500 cells/well depending on cell lines) were cultured overnight in 96-well plates. Cell viability was assessed after the addition of DCC-2701 or vehicle control at the indicated concentrations for 72 hr using the CellTiter Blue Cell Viability Assay reagent (Promega, Madison, WI). The number of viable cells was assessed by the determination of a fluorescent end product (resorufin) at 590 nm as a result of conversion of a redox dye (resazurin) by living cells for 3 hr using a fluorescent Infinite 200 PRO plate reader (Tecan US, Inc., Morrisville, NC).

Measurement of HGF concentration by ELISA

Tumor cells and fibroblasts were grown in 24-well Transwell plates as described above in cell migration assay. Cell culture media (50 μl) from the lower wells were centrifuged at 10,000x g for 15 min to remove cell debris and examined for HGF levels using the Quantikine Human HGF ELISA kit (R & D Systems) according to manufacturer's instructions.

Immunoblot analysis

Cells were cultured as indicated and lysed using radioimmunoprecipitation assay buffer (50 mM Tris HCl, pH 8.0, 5 mM EDTA, 150 mM NaCl, 1% NP40, 0.5% sodium deoxycholate, and 0.1% SDS) supplemented with both protease inhibitor cocktails (Roche Diagnostics Corporation, Indianapolis, IN) and phosphatase inhibitor cocktails (Thermo Fisher Scientific, Rockford, IL). Equal amount of denatured proteins (30 μg per lane) were separated by SDS-PAGE and subjected to immunoblotting as described previously (25). Protein detection was achieved using Western Lightning TM Plus-ECL Enhanced Chemiluminescence Substrate (Bio-Rad, Hercules, CA).

DCC-2701 Efficacy in an *In Vivo* Xenograft Mouse Model

All procedures were performed following the guidelines adopted by the Animal Care and Use Committee of the University of Kansas Medical Center. Female athymic nude mice (NCr-*nu/nu* 8 weeks old) were purchased from Charles River. Five million SKOV3 cells in PBS mixed with an equal volume of cold BD Matrigel™ Matrix High Concentration (BD Biosciences, San Jose, CA, USA) were inoculated subcutaneously into the right flank of each mouse. When tumor volumes reached approximately 100 mg on average at 2 weeks, mice were randomly assigned to 4 groups and were treated as follows: 0.4% hydroxypropyl methylcellulose vehicle control, oral gavage, once daily (n=10) or with DCC-2701 at 5, 10 or 20 mg/kg, oral gavage, once daily (n=10/arm). The treatment lasted 28 days, and tumor volume and body weight were measured every 2 or 3 days, respectively. Tumor volume in mg is calculated by the following formula: volume = (length × width^2/2).

Indirect immunofluorescence staining

Tissue microarrays (TMAs) contain two independent 1 mm cores per normal ovary or tumor were obtained and evaluated under a protocol approved by the KUMC institutional review board. TMAs were subject to immunofluorescence staining to evaluate HGF expression levels in the stroma of normal ovaries and tumors. Sections of TMAs were deparaffinised and incubated with primary antibody (anti-HGF antibody, R & D systems) and secondary antibody as described (25) after antigen retrieval treatment and blocking procedure. HGF expression was visualized using Nikon 80i fluorescent microscope.

Statistical analyses

Two sample Wilcoxon rank sum tests (equivalent to the Mann-Whitney test) were performed to examine if cell migration rates were changed (induced and/or suppressed) by treatments compared to untreated condition (as shown in Figures 1a, 2c, 2d, and 6c) using R (version 2.15.1). Two-way analysis of variance was conducted to determine if there were significant effect of fibroblasts (ECMs), cancer cell and their interaction on secreted HGF levels (used in Figure 2a). In order to examine the effect of DCC-2701 treatment on tumor burden, one-way analysis of variance was performed with post-hok analysis by the method of Shapiro-Wilk. P-values smaller than 0.05 were considered significant.

Supplementary Material

Refer to Web version on PubMed Central for supplementary material.

ACKNOWLEDGEMENTS

REFERENCES

1. Siegel R, Naishadham D, Jemal A. Cancer statistics, 2013. CA: a cancer journal for clinicians. 2013; 63(1):11–30. [PubMed: 23335087]

2. Ozols RF, Bookman MA, Connolly DC, Daly MB, Godwin AK, Schilder RJ, et al. Focus on epithelial ovarian cancer. Cancer Cell. 2004; 5(1):19–24. [PubMed: 14749123]

3. Bhowmick NA, Moses HL. Tumor-stroma interactions. Curr Opin Genet Dev. 2005; 15(1):97–101. [PubMed: 15661539]

4. Liotta LA, Kohn EC. The microenvironment of the tumour-host interface. Nature. 2001; 411(6835): 375–379. [PubMed: 11357145]

5. Beacham DA, Cukierman E. Stromagenesis: the changing face of fibroblastic microenvironments during tumor progression. Semin Cancer Biol. 2005; 15(5):329–341. [PubMed: 15970443]

6. Hynes RO. The extracellular matrix: not just pretty fibrils. Science. 2009; 326(5957):1216–1219. [PubMed: 19965464]

7. Matsumoto K, Nakamura T. Hepatocyte growth factor and the Met system as a mediator of tumor-stromal interactions. Int J Cancer. 2006; 119(3):477–483. [PubMed: 16453287]

8. Sierra JR, Tsao MS. c-MET as a potential therapeutic target and biomarker in cancer. Ther Adv Med Oncol. 2011; 3(1 Suppl):S21–S35. [PubMed: 22128285]

9. Corps AN, Sowter HM, Smith SK. Hepatocyte growth factor stimulates motility, chemotaxis and mitogenesis in ovarian carcinoma cells expressing high levels of c-met. Int J Cancer. 1997; 73(1): 151–155. [PubMed: 9334823]

10. Taipale J, Keski-Oja J. Growth factors in the extracellular matrix. Faseb J. 1997; 11(1):51–59. [PubMed: 9034166]

11. Tatsumi R, Allen RE. Active hepatocyte growth factor is present in skeletal muscle extracellular matrix. Muscle Nerve. 2004; 30(5):654–658. [PubMed: 15389661]

12. Comoglio PM, Giordano S, Trusolino L. Drug development of MET inhibitors: targeting oncogene addiction and expedience. Nat Rev Drug Discov. 2008; 7(6):504–516. [PubMed: 18511928]

13. Straussman R, Morikawa T, Shee K, Barzily-Rokni M, Qian ZR, Du J, et al. Tumour micro-environment elicits innate resistance to RAF inhibitors through HGF secretion. Nature. 2012; 487(7408):500–504. [PubMed: 22763439]

14. Wilson TR, Fridlyand J, Yan Y, Penuel E, Burton L, Chan E, et al. Widespread potential for growth-factor-driven resistance to anticancer kinase inhibitors. Nature. 2012; 487(7408):505–509. [PubMed: 22763448]

15. Ayhan A, Ertunc D, Tok EC, Ayhan A. Expression of the c-Met in advanced epithelial ovarian cancer and its prognostic significance. Int J Gynecol Cancer. 2005; 15(4):618–623. [PubMed: 16014115]

16. Zillhardt M, Christensen JG, Lengyel E. An orally available small-molecule inhibitor of c-Met, PF-2341066, reduces tumor burden and metastasis in a preclinical model of ovarian cancer metastasis. Neoplasia. 2010; 12(1):1–10. [PubMed: 20072648]

17. Zillhardt M, Park SM, Romero IL, Sawada K, Montag A, Krausz T, et al. Foretinib (GSK1363089), an orally available multikinase inhibitor of c-Met and VEGFR-2, blocks proliferation, induces anoikis, and impairs ovarian cancer metastasis. Clin Cancer Res. 2011; 17(12):4042–4051. [PubMed: 21551255]

18. Gordon MS, Sweeney CS, Mendelson DS, Eckhardt SG, Anderson A, Beaupre DM, et al. Safety, pharmacokinetics, and pharmacodynamics of AMG 102, a fully human hepatocyte growth factor-

neutralizing monoclonal antibody, in a first-in-human study of patients with advanced solid tumors. Clin Cancer Res. 2010; 16(2):699–710. [PubMed: 20068101]

19. Liu X, Newton RC, Scherle PA. Developing c-MET pathway inhibitors for cancer therapy: progress and challenges. Trends Mol Med. 2009; 16(1):37–45. [PubMed: 20031486]

20. Lyon M, Deakin JA, Mizuno K, Nakamura T, Gallagher JT. Interaction of hepatocyte growth factor with heparan sulfate. Elucidation of the major heparan sulfate structural determinants. The Journal of biological chemistry. 1994; 269(15):11216–11223. [PubMed: 8157651]

21. Ashikari S, Habuchi H, Kimata K. Characterization of heparan sulfate oligosaccharides that bind to hepatocyte growth factor. The Journal of biological chemistry. 1995; 270(49):29586–29593. [PubMed: 7494002]

22. Zioncheck TF, Richardson L, Liu J, Chang L, King KL, Bennett GL, et al. Sulfated oligosaccharides promote hepatocyte growth factor association and govern its mitogenic activity. The Journal of biological chemistry. 1995; 270(28):16871–16878. [PubMed: 7622503]

23. Flynn DL, Ahn YM, Berger MSTC, Hood MM, Kaufman MD, Lu W, Patt T, Samarakoon T, Smith BD, Turner BA, Vogeti L, Vogeti S, Wise SC. Rebastinib and DCC-2701: Targeting of resistance mechanisms in cancer treatment. ACS National Meeting, New Orleans, April 8, MEDI 209. 2013

24. Sawada K, Radjabi AR, Shinomiya N, Kistner E, Kenny H, Becker AR, et al. c-Met overexpression is a prognostic factor in ovarian cancer and an effective target for inhibition of peritoneal dissemination and invasion. Cancer Res. 2007; 67(4):1670–1679. [PubMed: 17308108]

25. Kwon Y, Cukierman E, Godwin AK. Differential expressions of adhesive molecules and proteases define mechanisms of ovarian tumor cell matrix penetration/invasion. PLoS One. 2011; 6(4):e18872. [PubMed: 21526198]

26. Furge KA, Zhang YW, Vande Woude GF. Met receptor tyrosine kinase: enhanced signaling through adapter proteins. Oncogene. 2000; 19(49):5582–5589. [PubMed: 11114738]

27. Pan BS, Chan GK, Chenard M, Chi A, Davis LJ, Deshmukh SV, et al. MK-2461, a novel multitargeted kinase inhibitor, preferentially inhibits the activated c-Met receptor. Cancer Res. 2010; 70(4):1524–1533. [PubMed: 20145145]

28. Ponzetto C, Bardelli A, Zhen Z, Maina F, dalla Zonca P, Giordano S, et al. A multifunctional docking site mediates signaling and transformation by the hepatocyte growth factor/scatter factor receptor family. Cell. 1994; 77(2):261–271. [PubMed: 7513258]

29. Michieli P, Basilico C, Pennacchietti S, Maffe A, Tamagnone L, Giordano S, et al. Mutant Met-mediated transformation is ligand-dependent and can be inhibited by HGF antagonists. Oncogene. 1999; 18(37):5221–5231. [PubMed: 10498872]

30. Miyata Y, Kanetake H, Kanda S. Presence of phosphorylated hepatocyte growth factor receptor/c-Met is associated with tumor progression and survival in patients with conventional renal cell carcinoma. Clin Cancer Res. 2006; 12(16):4876–4881. [PubMed: 16914575]

31. Marchand-Adam S, Marchal J, Cohen M, Soler P, Gerard B, Castier Y, et al. Defect of hepatocyte growth factor secretion by fibroblasts in idiopathic pulmonary fibrosis. Am J Respir Crit Care Med. 2003; 168(10):1156–1161. [PubMed: 12947024]

32. Matsuoka H, Sisson TH, Nishiuma T, Simon RH. Plasminogen-mediated activation and release of hepatocyte growth factor from extracellular matrix. Am J Respir Cell Mol Biol. 2006; 35(6):705–713. [PubMed: 16840775]

33. Lyon M, Deakin JA, Rahmoune H, Fernig DG, Nakamura T, Gallagher JT. Hepatocyte growth factor/scatter factor binds with high affinity to dermatan sulfate. The Journal of biological chemistry. 1998; 273(1):271–278. [PubMed: 9417075]

34. Nayeri F, Nayeri T, Aili D, Brudin L, Liedberg B. Clinical impact of real-time evaluation of the biological activity and degradation of hepatocyte growth factor. Growth Factors. 2008; 26(3):163–171. [PubMed: 18569024]

35. Hamilton TC, Young RC, McKoy WM, Grotzinger KR, Green JA, Chu EW, et al. Characterization of a human ovarian carcinoma cell line (NIH:OVCAR-3) with androgen and estrogen receptors. Cancer Res. 1983; 43(11):5379–5389. [PubMed: 6604576]

36. Langdon SP, Lawrie SS, Hay FG, Hawkes MM, McDonald A, Hayward IP, et al. Characterization and properties of nine human ovarian adenocarcinoma cell lines. Cancer Res. 1988; 48(21):6166–6172. [PubMed: 3167863]

37. Quiros RM, Valianou M, Kwon Y, Brown KM, Godwin AK, Cukierman E. Ovarian normal and tumor-associated fibroblasts retain in vivo stromal characteristics in a 3-D matrix-dependent manner. Gynecol Oncol. 2008; 110(1):99–109. [PubMed: 18448156]

38. Amatangelo MD, Bassi DE, Klein-Szanto AJ, Cukierman E. Stroma-derived three-dimensional matrices are necessary and sufficient to promote desmoplastic differentiation of normal fibroblasts. Am J Pathol. 2005; 167(2):475–488. [PubMed: 16049333]

39. Beacham DA, Amatangelo MD, Cukierman E. Preparation of extracellular matrices produced by cultured and primary fibroblasts. Chapter 10. Curr Protoc Cell Biol. 2007; (Unit 10):9. [PubMed: 18228495]

40. Castello-Cros R, Cukierman E. Stromagenesis during tumorigenesis: characterization of tumor-associated fibroblasts and stroma-derived 3D matrices. Methods Mol Biol. 2009; 522:275–305. [PubMed: 19247611]

41. Cukierman E, Pankov R, Stevens DR, Yamada KM. Taking cell-matrix adhesions to the third dimension. Science. 2001; 294(5547):1708–1712. [PubMed: 11721053]
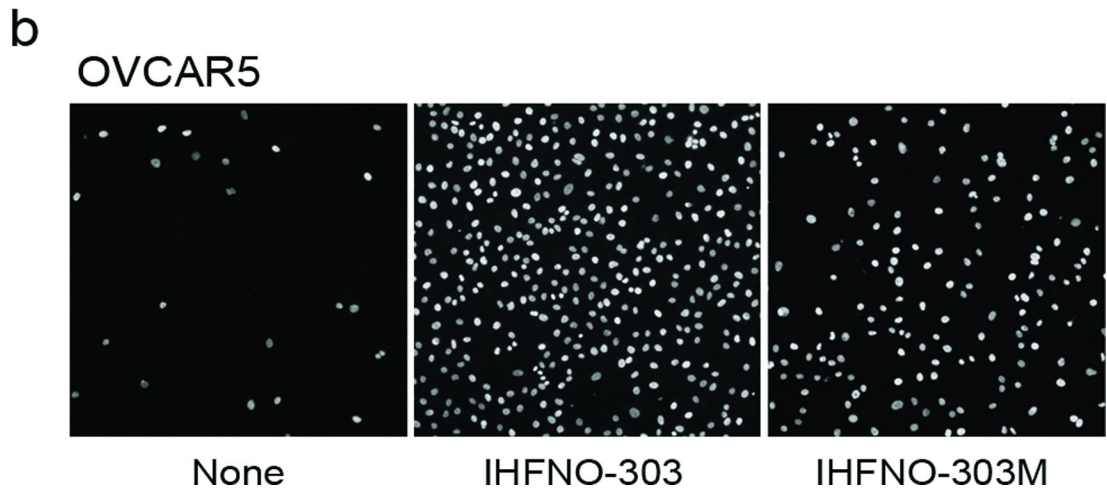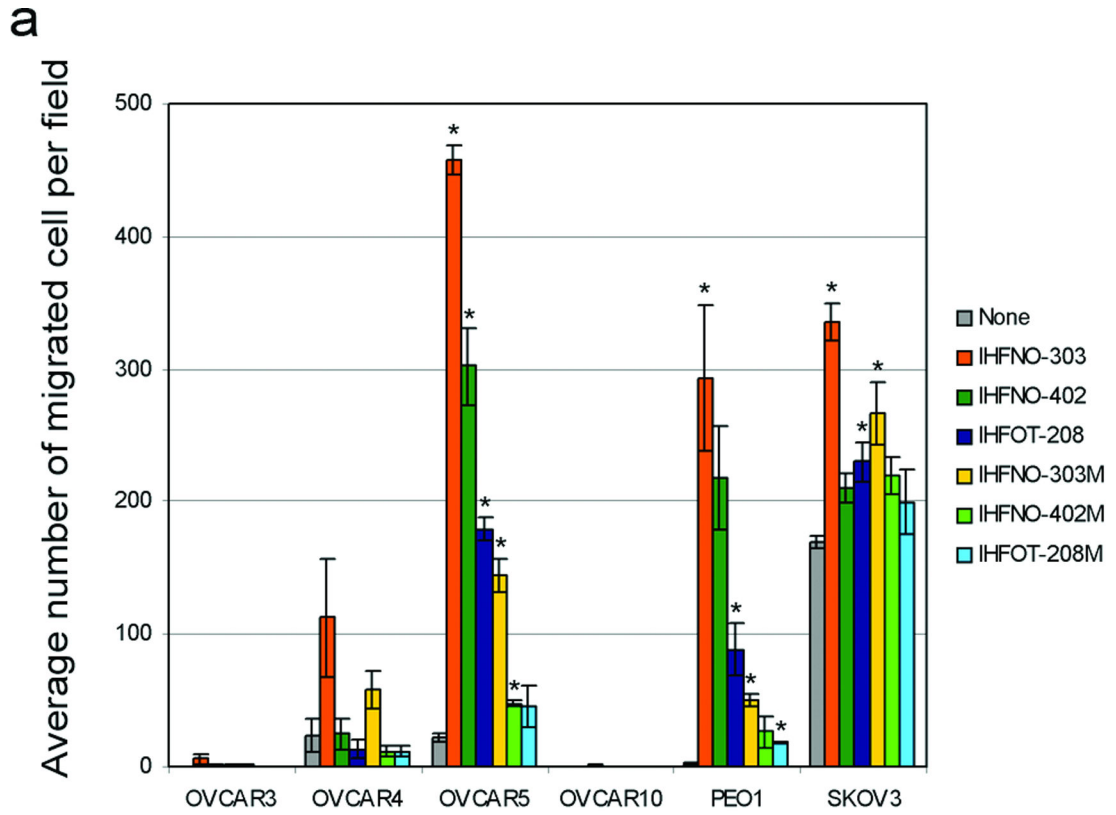
Author Manuscript

Author Manuscript

Author Manuscript

Author Manuscript

Figure 1.

Stimulation of ovarian cancer cell migration during the interaction with human ovarian fibroblasts and their derived ECMs. (a) Ovarian cancer cells (upper well) were allowed to migrate in the presence of ovarian fibroblasts and their derived ECMs (lower well) in Transwell plates. OVCAR3, OVCAR4, OVCAR5, PEO1, and SKOV3 cells increased their migration by the interaction with IHFNO-303 fibroblasts and/or their derived ECMs (IHFNO-303M). Migration of OVCAR5 and PEO1 cells was also stimulated by IHFNO-402 and IHFOT-208 fibroblasts. None of fibroblasts or ECMs increased the migration of

OVCAR10 cells. Average number of migrated cells per field ± S.E. is shown. Asterisks (*) represent significant differences ($p < 0.05$). (b) Images shown are representative of stained nuclei of OVCAR5 cells migrated under the indicated condition.
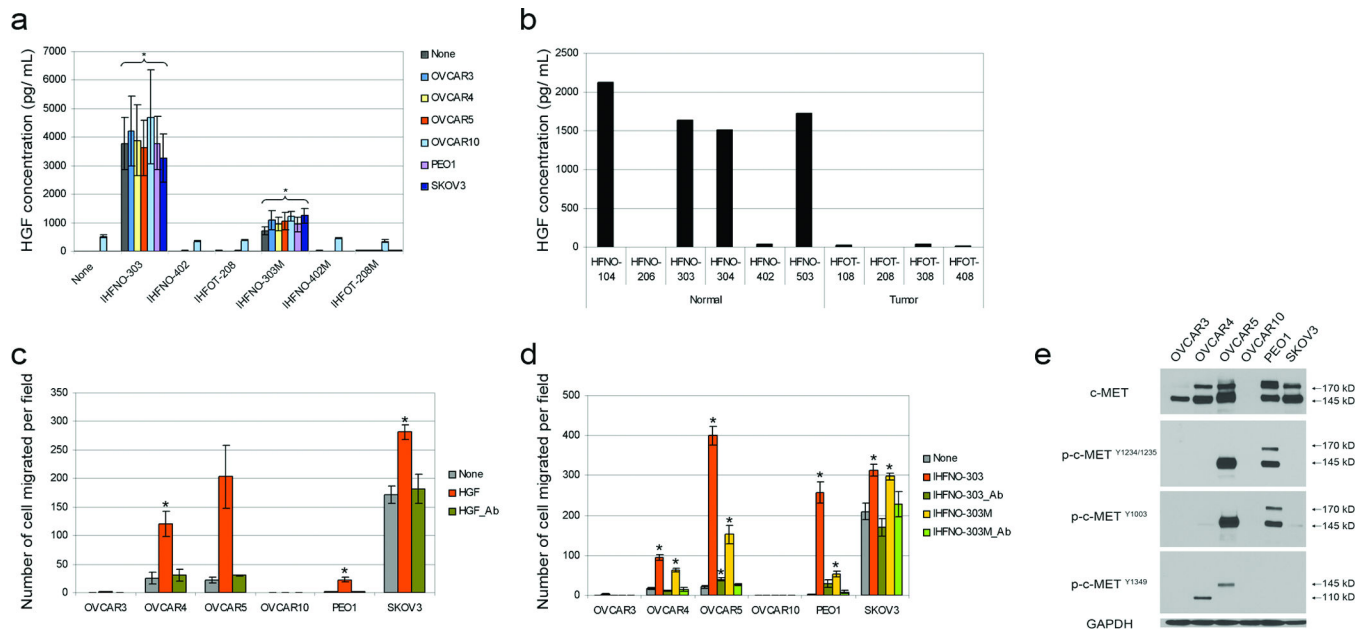
Figure 2.
Increase of ovarian cancer cell migration by fibroblast-derived HGF. (a) HGF levels were measured from fibroblast- and ECM-derived conditioned media in the presence and absence of cancer cells by ELISA. Culture media did not contain detectable level of HGF. Asterisks (*) represent significant differences ($p < 0.05$) among different fibroblasts and their derived ECMs. (b) HGF levels were similarly measured as described in (a) from primary fibroblasts derived from normal ovaries (HFNO-) and ovarian tumors (HFOT-). (c) Recombinant human HGF (100 ng/mL) promoted migration of OVCAR3, OVCAR4, OVCAR5, and PEO1 but not OVCAR10 cells. Cell migration induced by HGF was prevented by a HGF neutralizing antibody (1 μg/mL). (d) IHFNO-303 fibroblast and its derived ECMs, IHFNO-303M, stimulated ovarian cancer cell migration and this increase of migration was effectively inhibited by a HGF neutralizing antibody (1 μg/mL). (e) OVCAR3, OVCAR4, OVCAR5, PEO1, and SKOV3 that increased migration in response to HGF expressed c-MET but OVCAR10 cells, irresponsive to HGF did not express c-MET. c-MET corresponding to 170kD and 145 kD is pro-form and mature form, respectively. Non-specific band (110 kD) was also detected using the antibody for phosphorylated c-MET on Tyr[1349].
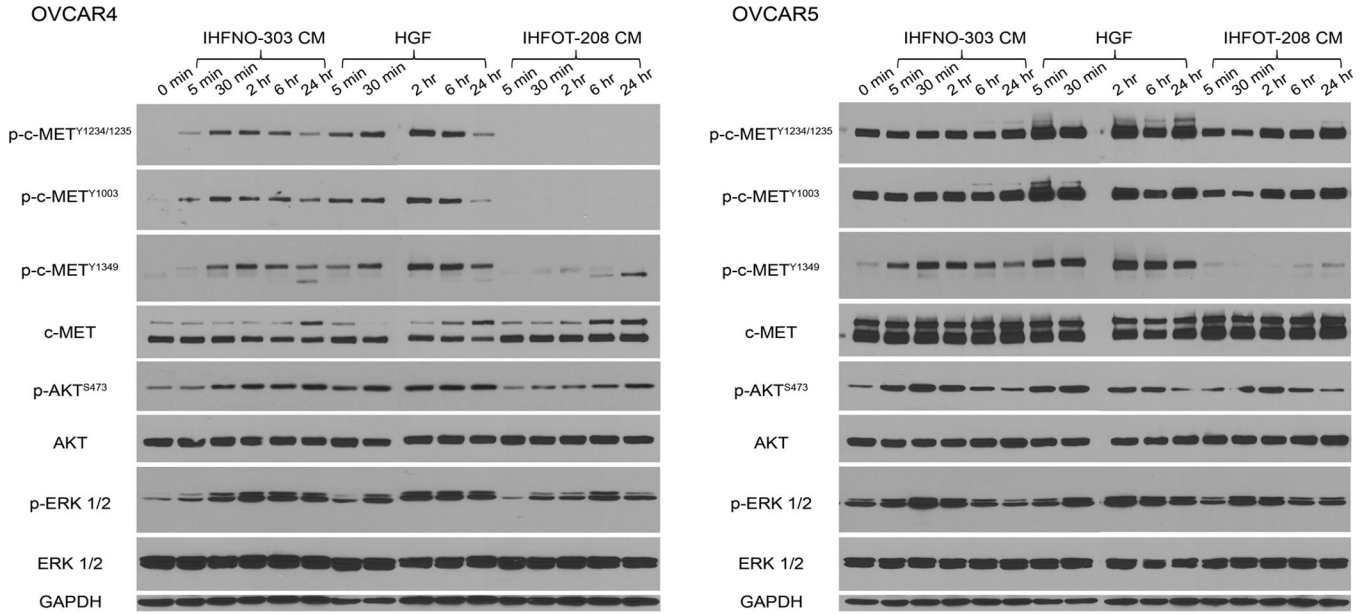
Figure 3.
Induction of c-MET mediated signal transduction by conditioned media derived from
IHFNO-303 fibroblast and recombinant HGF. In OVCAR4 cells that do not express
phosphorylated c-MET without HGF, both fibroblast HGF and recombinant HGF similarly
induced phosphorylation of c-MET on all phosphorylation sites, $Tyr^{1234/1235}$. Tyr^{1003}, and
Tyr^{1349} and subsequently increased phosphorylation of c-MET downstream signaling
molecules, AKT and ERK. In OVCAR5 cells that possess constitutive c-MET
phosphorylation, fibroblast HGF only increased the phosphorylation of c-MET on Tyr^{1349}
without affecting the other sites, $Tyr^{1234/1235}$ and Tyr^{1003}. Increase of phosphorylation of
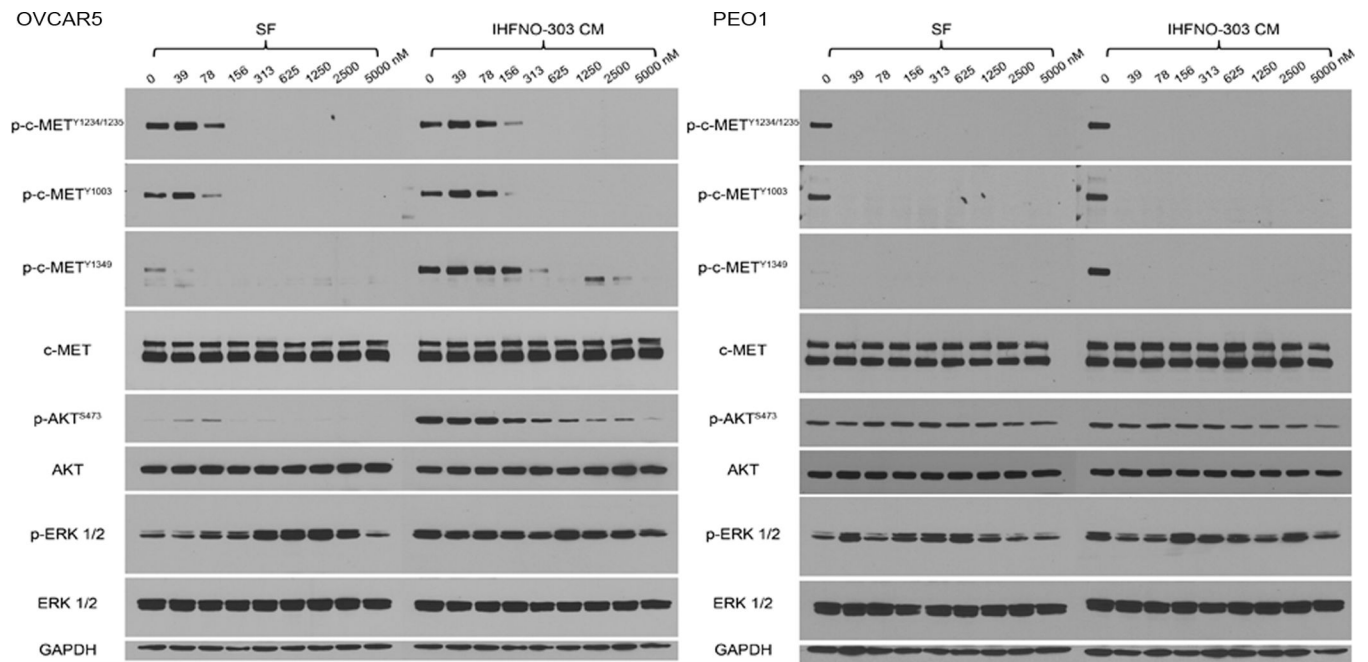Tyr^{1349} was accompanied by enhanced activation of downstream signaling.

Figure 4.
Effect of DCC-2701 on constitutive and induced c-MET phosphorylation and c-MET downstream signaling. OVCAR5 and PEO1 cells were cultured in serum free (SF) media (constitutive) or IHFNO-303 CM (induced) that contain DCC-2701 in a concentration range between 0 to 10 μM. DCC-2701 effectively suppressed constitutive and IHFNO-303 CM-induced c-MET phosphorylation.
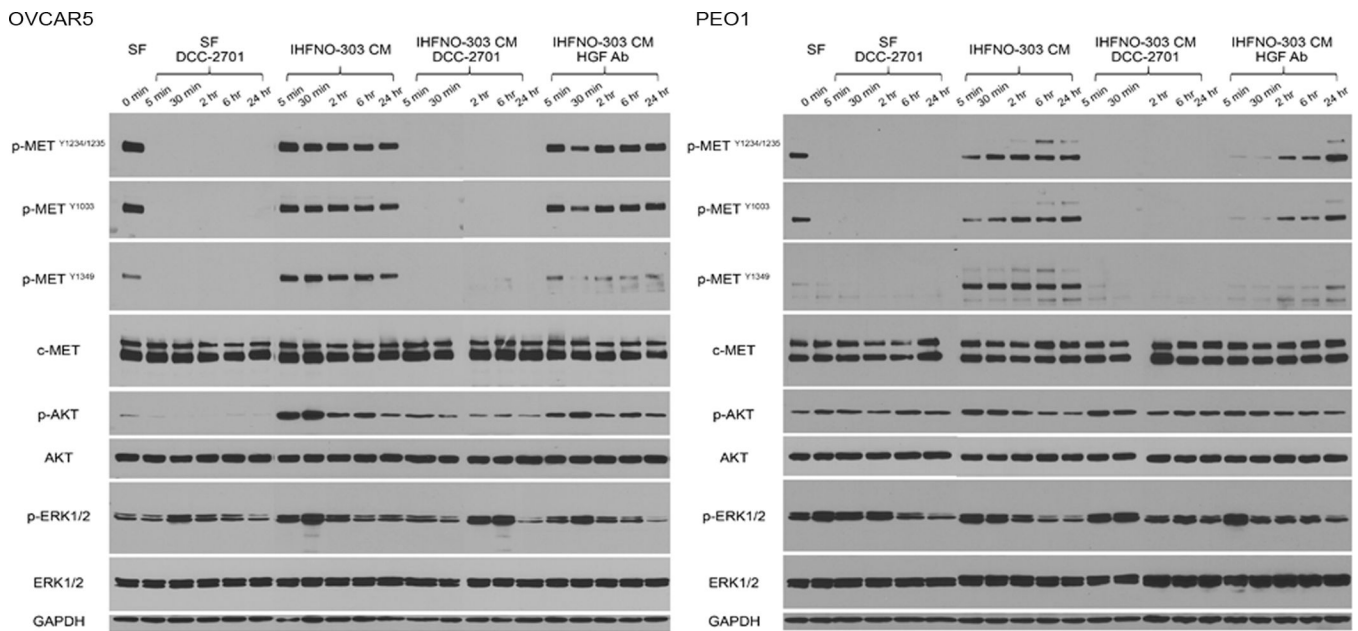
Figure 5.
Effect of DCC-2701 on constitutive and induced c-MET phosphorylation and c-MET downstream signaling during 24 hr of treatment. OVCAR5 and PEO1 cells were cultured in serum free media (constitutive) or IHFNO-303 CM (induced) containing DCC-2701 (2.5 μM). Inhibitory effect of DCC-2701 lasted for 24 hr and treatment of DCC-2701 suppressed the induction of c-MET and its downstream activation. In comparison, a HGF neutralizing antibody (2.5 μg/mL) did not effectively inhibit phosphorylation of c-MET and downstream signaling transducers.
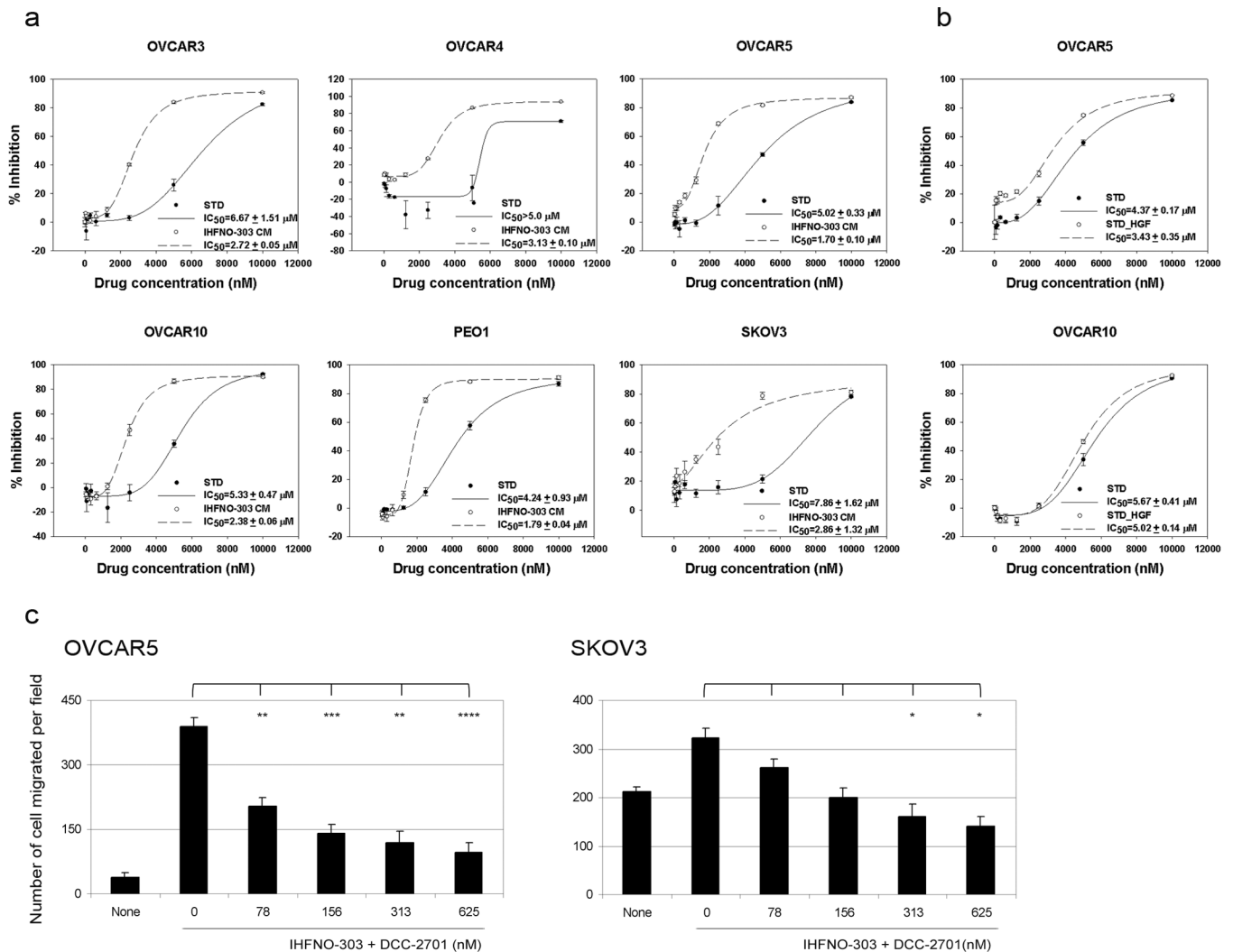
Figure 6.
Effect of DCC-2701 on ovarian cancer cell viability and migration. (a) Ovarian cancer cells were cultured in 96-well plates overnight and media were replaced with standard media or IHFNO-303 CM containing DCC-2701 in a range of 0 (vehicle control) to 10 μM and grown for an additional 72 hrs. Cell growth was measured using CellTiter Blue reagent. Cell viability relative to vehicle control (% inhibition) is shown. DCC-2701 more effectively inhibited cell viability when exposed to fibroblast condition media (IHFNO-303 CM) relative to media alone. (b) OVCAR5 and OVCAR10 cells that represent c-MET positive and negative cells, respectively, were plated overnight. Media were replaced with freshly prepared standard media or the media supplemented with recombinant HGF containing different concentrations of DCC-2701. Cell viability was estimated as described in (a). (c) OVCAR5 and SKOV3 cells were pretreated with DCC-2701 at the indicated concentration for 1 hr and were allowed to migrate for 24 hr in the presence/absence of IHFNO-303 fibroblast in Transwell plates. Average number of migrated cells per field ± S.E. is shown. Compared with (IHFNO-303 plus no drug), *p < 0.05, **p < 0.01, ***p < 0.001, ****p < 0.0005 (n=3; using Wilcoxon rank sum test).
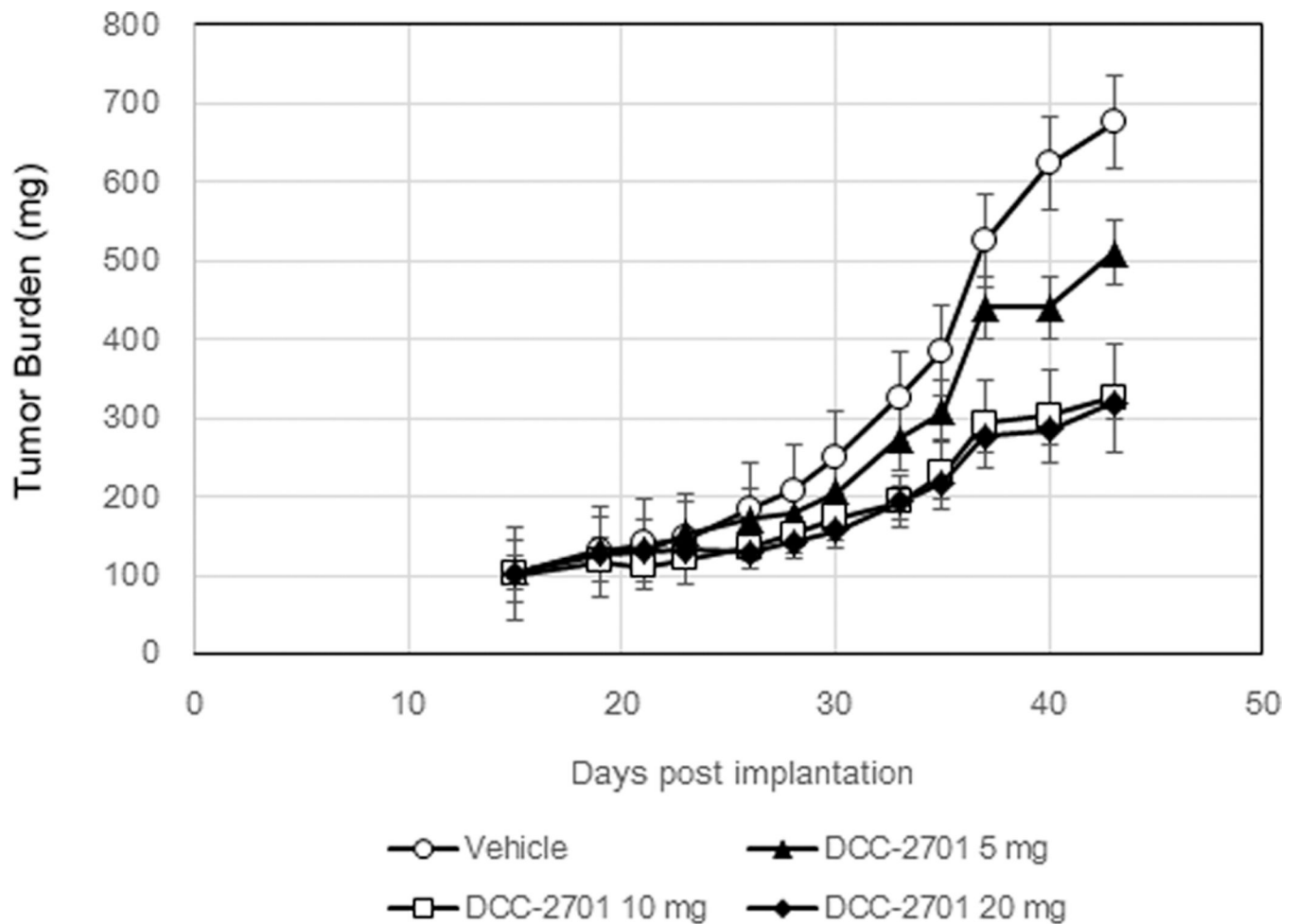
Figure 7

Figure 7.
Anti-tumor effects of DCC-2701 in a xenograft nude mouse model of ovarian cancer. SKOV3 cells were implanted on the right flank of each mouse and tumor volume was measure twice a week using a caliper. Vehicle control or different dose of DCC-2701 was administered daily by oral gavage after the tumor volume reached about 100 mg (at 2 weeks after cell implantation). The mean tumor burdens (mg, $(L \times W^2)/2$, L and W are orthogonal tumor length and width, respectively) $\pm$ S.E. are shown. The final tumor burden of groups treated with 10 and 20 mg/kg of DCC-2701 for 28 days was significantly lower ($p < 0.05$) compared to the vehicle treated group. One mouse in the DCC-2701 treatment group at 10 mg/kg was removed from the analysis due to an inadvertent death related to the oral gavage.